Journal of Fluorescence, Vol. 11, No. 4, December 2001 (© 2002)

Inter- and Intramolecular Dynamics of Pyrenyl Lipids in Bilayer Membranes from Time-Resolved Fluorescence Spectroscopy

Eugene G. Novikov[1] and Antonie J. W. G. Visser[2–4]

The analysis of time-resolved fluorescence of monopyrenyl phospholipid monomer and excimer emission is reviewed using a model based on the diffusion equation for bimolecular reactions in two-dimensional planar membrane bilayers. This aspect is illustrated by the analysis of a real experiment. The method can also be extended to short-range diffusion, which can be measured for dipyrenyl phospholipids in membrane bilayers. The latter aspect is illustrated by the analysis of a simulated experiment to show the experimental requirements to recover the desired parameters.

KEY WORDS: Pyrene monomer and excimer; time-resolved fluorescence; translation diffusion; membrane bilayer; vesicles; liposomes.

INTRODUCTION

Pyrene-containing phospholipids report on the lateral mobility of these lipids in bilayer membranes because of the ability of forming excimers, when one pyrene molecule in the excited state collides with another one in the ground state [1]. The excimer fluorescence is at longer wavelengths than the monomer fluorescence. The ratio of excimer-to-monomer emission intensities (E/M ratio) is a measure of the rate of excimer formation, which is determined by the frequency of collisions between pyrene moieties and hence can be related to parameters describing membrane dynamics and organization (for reviews see Refs. 2 and 3, and for a pictorial view of all aspects see Fig. 1). In short, the E/M ratio is indicative of the "microfluidity" of the membrane, since the dynamic properties of the local probe environment are investigated: the higher this ratio, the more fluid the membrane. The dynamic processes governing the excimer formation have been modeled with a lattice or "milling crowd" model, which considers lipid probes migrating in a trigonal lattice of lipids by exchanging positions with one of their six neighbors [4–6]. This lateral diffusion is over an intermediate to long range, covering a distance of the order of magnitude of tens to hundreds of nanometers. Instead of measuring steady-state E/M ratios, time-resolved fluorescence techniques can also be utilized to determine diffusion coefficients of pyrene-containing lipids in membranes using a model of diffusion-controlled bimolecular reactions in two dimensions derived in the mid-1970s by Razi Naqvi [7]. The validation of the latter model in the case of long-range diffusion has been done using time-resolved fluorescence applied to monopyrenylphosphatidylcholine [$pyr_{10}PC$; 1-palmitoyl-2-(pyrenodecanoyl)-*sn*-glycero-3-phosphocholine (see Fig. 1D)] in 1-palmitoyl-2-oleoyl-phosphatidylcholine (POPC) vesicles [8]. The approach developed in Ref. 8 has been

[1] Institut Curie, INSERM U350, Bât. 112, Centre Universitaire, 91405 Orsay Cedex, France.
[2] MicroSpectroscopy Centre, Laboratory of Biochemistry, Wageningen University, Dreijenlaan 3, 6703 HA Wageningen, The Netherlands.
[3] Department of Structural Biology, Institute of Molecular Biological Sciences, Vrije Universiteit, Amsterdam, The Netherlands.
[4] To whom correspondence should be addressed at MicroSpectroscopy Centre, Laboratory of Biochemistry, Wageningen University, Dreijenlaan 3, 6703 HA Wageningen, The Netherlands.

1053-0509/01/1200-0297/0 © 2002 Plenum Publishing Corporation

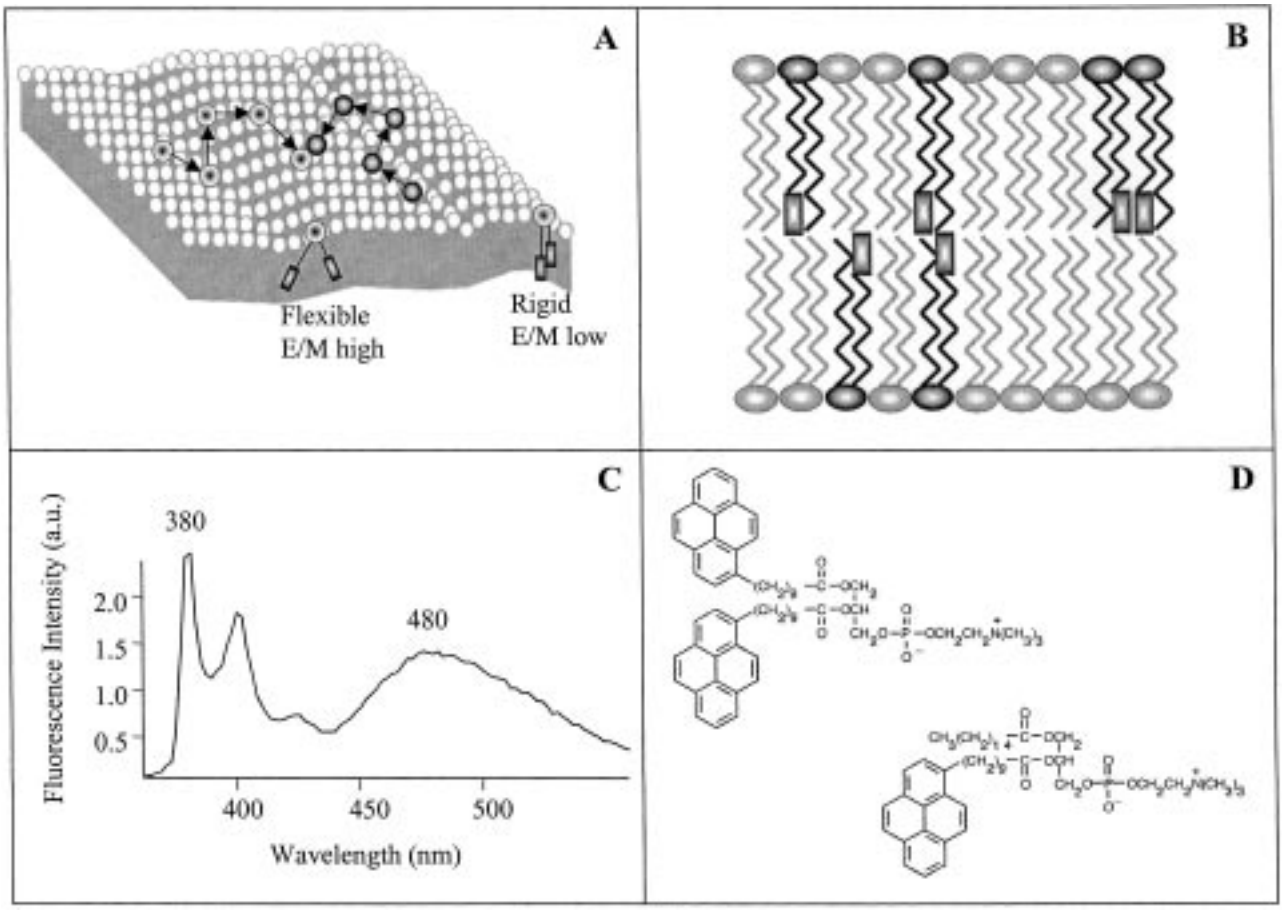

Fig. 1. (A) Schematic view of long-range lateral diffusion of two monopyrene (phospho-) lipid molecules at the surface of the membrane (one excited and one not) leading to collision and excimer formation. Also shown is the short-range motion of a dipyrenyl lipid, which reports on the microfluidity near the probe lipid. (B) Excimers can also be formed between monopyrene lipids residing in both parts of the bilayer. (C) An example of monomer and excimer emission spectra taken from dipyrenedecanoylphosphatidylcholine (dipyr$_{10}$PC) in dioleoylphosphatidylcholine (DOPC) vesicles. (D) Chemical structures of monopyr$_{10}$PC and dipyr$_{10}$PC.

extended by global analysis of both monomer and excimer emission decays, thereby linking the common parameters [9]. As the model developed by Razi Naqvi [7] contains a number of parameters that are highly correlated, physically meaningful values of the different parameters have been critically assessed [9].

The collision between two pyr$_{10}$PC's is an intermolecular event and reports on lateral diffusion of this probe lipid dispersed in liposomes. On the other hand, dipyrenylphosphatidylcholine [two pyrene acyl chains are bound at the *sn*1 and *sn*2 positions in a phospholipid (see Fig. 1D)] forms excimers intramolecularly. This short-range diffusion, which actually is a motion over a short distance, of the order of the diameter of one or two phospholipids, is directly related to the motional freedom and the reorientational dynamics of the pyrene chains in the membrane. The E/M ratio then gives information on the local fluidity in a bilayer (see Fig. 1A). Changes in fluidity of membranes can then be detected via the intramolecular collision frequency of such dipyrenylphosphatidylcholines. These probes are highly sensitive to constraints imposed by their environment and can therefore be used as fluidity sensors for interior regions of bilayer membranes. By using both pyrenyl groups at different depths with respect to the glycerol moiety of the phospholipid, the fluidity can be measured at different depths in the membrane. Dipyrenylphosphatidylcholines have been widely used in membrane research [10–16]. The advantage is that they can be incorporated at a very low concentration (the typical probe/lipid mole fraction is circa 0.1%), which minimizes the possible perturbation of the host membrane.

The aim of the present is twofold. One aspect is concerned with the parametric modeling of the fluores-

cence kinetics of monomer and excimer emissions of pyr_{10} PC in bilayer membranes to obtain the lateral diffusion coefficients. This point is summarized and illustrated with experimental data obtained previously [9]. The other aspect is to show that local diffusion coefficients of dipyrenylphosphatidylcholine in bilayer membranes can be determined from global analysis of the time-resolved fluorescence of the pyrene monomer and excimer emissions, similarly as obtained for the lateral diffusion of monopyrenylphosphatidylcholine. This is illustrated by simulated experiments, which provide us with the required experimental accuracy that is needed to obtain physically meaningful parameters.

GLOBAL ANALYSIS OF TIME-RESOLVED FLUORESCENCE OF MONOMER AND EXCIMER EMISSIONS OF MONOPYRENYLPHOSPHATIDYLCHOLINE IN BILAYER MEMBRANES

Models. The model for monomer and excimer emission is based on the general reaction scheme depicted in Scheme I. The monomer M*, being excited by an infinitely narrow optical pulse $\delta(t)$, can undergo a reaction in the excited state with an unexcited monomer, M, thus forming the (excited) excimer E*. The time-dependent rate of this reaction is denoted $k(t)$. Excited monomers and excimers can relax to the ground state, emitting light with rate constants $1/\tau_M$ and $1/\tau_E$, respectively. While relaxing to the ground state the excimer is dissociated into two monomers.

The monomer fluorescence intensity decay, excited by an infinitely narrow optical pulse, is given by [17,18]

$$M(t) = M_0 \exp\left\{-\frac{t}{\tau_M} - \int_0^t k(x)dx\right\} \quad (1)$$

where M_0 is the fluorescence intensity at zero time ($t = 0$), τ_M is the monomer fluorescence decay time, and $k(x)$ is the time-dependent reaction rate coefficient, derived from the analytical solution of the diffusion equation [19], subject to Collins and Kimball boundary conditions and uniform initial conditions [7]:

$$k(x) = \frac{16Dh^2c}{\pi} \int_0^\infty \frac{\exp\{-2\,Dxu^2/R^2\}}{u[(hJ_0(u) + uJ_1(u))^2 + (hY_0(u) + uY_1(u))^2]}\,du \quad (2)$$

where $h = \kappa R/D$, J_v, and Y_v are Bessel functions of the first and second kind, respectively, of order v, c is the concentration of the excimer probe (molecules per area), D is the diffusion coefficient of one reactant, R is the reaction distance, and κ is the intrinsic reaction rate constant. When $\kappa \to \infty$ reaction always occurs at contact, and when $\kappa \to 0$ reaction never occurs [17]. The excimer fluorescence intensity decay is represented by a convolution of the monomer decay and its own monoexponential excimer decay law [17,20]:

$$E(t) = k(t)M(t) \otimes \exp\{-t/\tau_E\} \quad (3)$$

where $\otimes$ denotes convolution and τ_E is the fluorescence decay time of the excimer.

Analysis. To avoid distortions connected to the wavelength dependence of the detecting path, analysis has been performed by the reference reconvolution method [21], where the observed detected decay is represented via the monoexponential decay of a reference com-

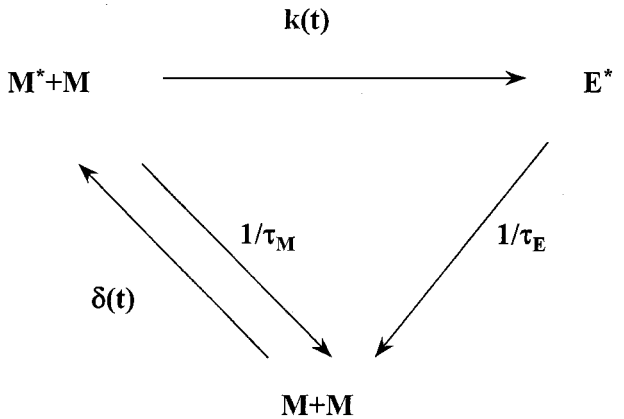

Scheme 1. Scheme describing the pyrene excimer reaction.

pound, which emits light at the same wavelength as the investigated samples (POPOP in this case). Applying the reference reconvolution method to the analysis of monomer and excimer fluorescence decays leads to

$$F_M(t) = F_R(t) \otimes \{M'(t) + M(t)/\tau_R\} + F_R(t)M(0) \quad (4)$$

$$F_E(t) = F_R(t) \otimes \{E'(t) + E(t)/\tau_R\} + F_R(t)E(0) \quad (5)$$

where $F_R(x)$ and τ_R are the fluorescence decay function and decay time of the reference compound, respectively, and $M'(t)$ and $E'(t)$ are the first-order time derivatives of monomer and excimer decay laws, respectively.

After combining Eqs. (1) and (4) the detected decay for the monomer via the fluorescence decay of the reference compound is obtained:

$$F_M(t) = F_R(t) \otimes \{(\tau_R^{-1} - \tau_M^{-1} - k(t))M(t)\} + M_0F_R(t) \quad (6)$$

From Eqs. (3) and (5), the detected excimer fluorescence profile is obtained as

$$F_E(t) = F_R(t) \otimes \{(\tau_R^{-1} - \tau_E^{-1})E(t) + k(t)M(t)\} \quad (7)$$

The fit of the monomer and excimer fluorescence decay parameters was based on the Marquardt nonlinear method of least squares, described in detail elsewhere [22]. Since the time-dependent reaction rate coefficient $k(t)$ is equally present in the models for monomer [Eq. (1)] and excimer [Eq. (3)] emissions, the parameters characterizing $k(t)$ (i.e., concentration c, diffusion coefficient D, and intrinsic reaction rate constant κ) are the same for both decays. This implies the necessity of a global parametric fit of the fluorescence decay curves of monomer [Eq. (6)] and excimer [Eq. (7)] emission, assuming that the common parameters are equal for both curves. The reaction radius R was fixed to a value of 7.1×10^{-8} cm, obtained from Refs. 8 and 23 for two pyrene molecules. The goodness of fit was judged by χ^2 criteria, visual inspection of the residuals between experimental and fitted curves, and the autocorrelation function of residuals. The error estimation of the recovered parameters was performed by the exhaustive search method [24].

Example. As stated above, parameters such as the concentration, diffusion coefficient, and intrinsic reaction rate constant must always be the same for the monomer and excimer emissions of one membrane sample and therefore must be linked in the fitting procedure. The parameters that were not linked are the monomer and excimer decay times, since they may reflect kinetically different processes deactivating the excited state which cannot be resolved, and, of course, scaling factors for monomer and excimer emission intensities. A typical example of experimental and fitted decay curves is presented in Fig. 2 [for $pyr_{10}PC$ in dioleoylphosphatidylcholine (DOPC) liposomes]. The fitted curves show an acceptable quality, and therefore, the applicability of the model is justified. The parameters recovered after global analysis are given in the legend to Fig. 2. The diffusion coefficient D obtained is similar to that found by other methods such as FRAP [25], NMR [26], ESR [27], and single-molecule tracking [28,29]. The estimates for the global parameters are 3.1×10^{12} mol cm^{-2} for the concentration and 3720 cm s^{-1} for the intrinsic reaction rate. The latter observation indicates a finite (albeit rather high) reactivity of both reactants. In other words, there is a certain probability that the two reactants will not form an excimer upon contact.

INTRAMOLECULAR DYNAMICS OF DIPYRENYL LIPIDS IN BILAYER MEMBRANES FROM TIME-RESOLVED FLUORESCENCE SPECTROSCOPY

Models. The monomer fluorescence intensity decay, excited by an infinitely narrow optical pulse, is given by

$$M(t) = \exp\{-t/\tau_M\}S(t) \quad (8)$$

where $S(t)$ is the quenching survival probability, i.e., the probability that the excited state of the fluorophore generated at $t = 0$ has not been quenched by time t, and τ_M is the monomer fluorescence decay time.

The survival probability $S(t)$ is derived from a model for diffusion-mediated intramolecular fluorescence quenching based on the analytical solution of the Smoluchowski differential equation [30–32]. It is assumed that quenching occurs with a finite intrinsic reaction rate constant κ at the distance of closest approach R (reaction radius) between the reactants. At the distance of maximal separation R_{max}, the boundary is closed. The probability distribution density of the initial separation between the ends of both pyrene moieties is assumed to be uniform. In two dimensions, the survival probability $S(t)$ is given by

$$S(t) = \sum_{n=0}^{\infty} \alpha(\lambda_n) \exp\{-\lambda_n^2 Dt\}/\lambda_n \times \{R[J_{-1}(\lambda_n R) + \gamma(\lambda_n)Y_{-1}(\lambda_n R)] - R_{max}[J_{-1}(\lambda_n R_{max}) + \gamma(\lambda_n)Y_{-1}(\lambda_n R_{max})]\} \quad (9)$$

where D is the diffusion coefficient; J_v and Y_v are Bessel functions of the first and second kind, respectively, of order v; and the coefficients λ_n, $\gamma(\lambda_n)$, and $\alpha(\lambda_n)$ are determined from the initial and boundary conditions. Admissible values for λ are the roots of the following transcendental equation:

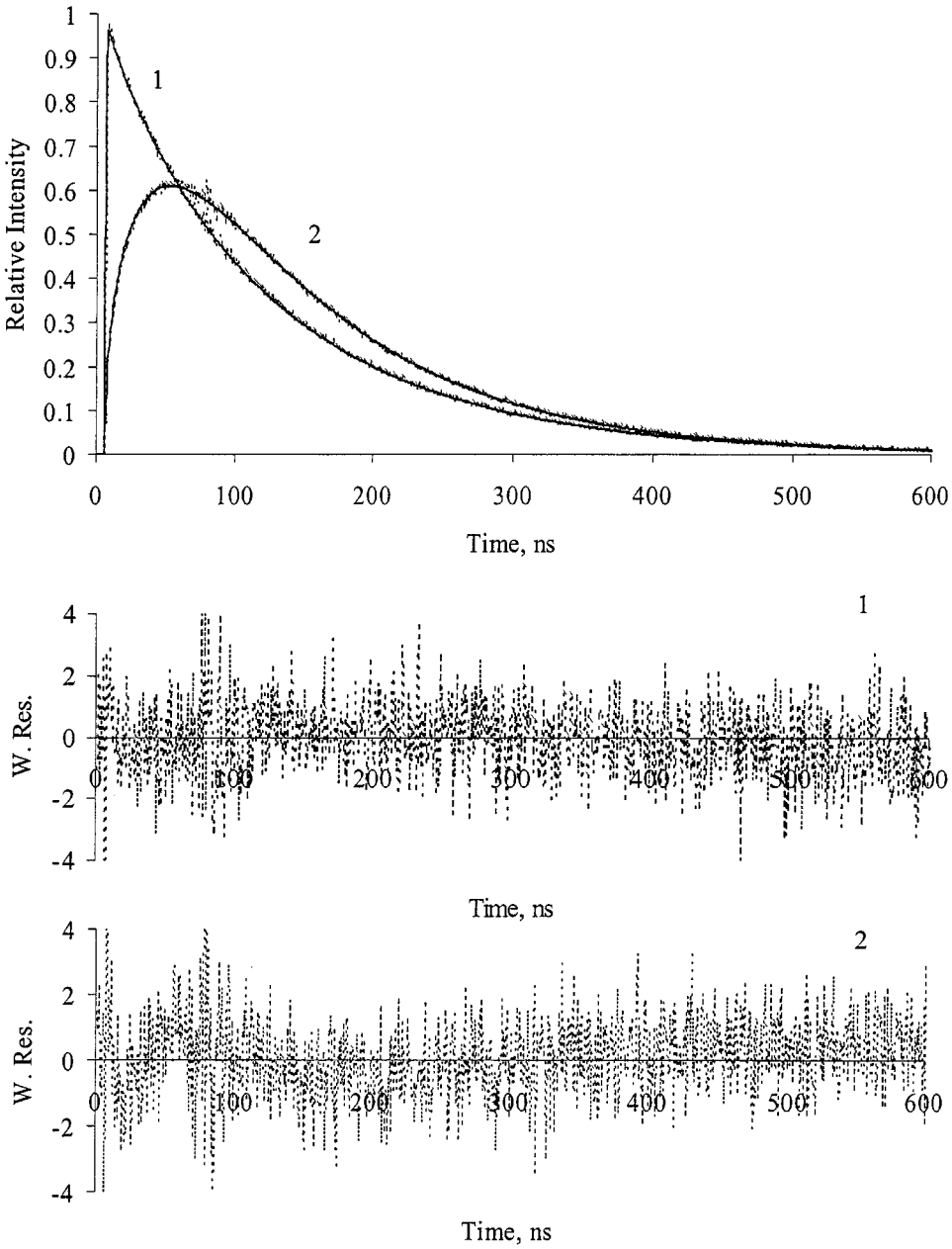

Fig. 2. Reference reconvolution of the time dependence of the monomer (curve 1) and excimer (curve 2) fluorescence of $pyr_{10}PC$ in liposomes made from DOPC at 20°C. The probe:phospholipid molar ratio was 1:150. The experimental curves are represented by points and the fitted curves by solid lines. The weighted residuals (W. Res.) for both globally analyzed curves are also shown. Recovered parameters: $D = 7.2 \times 10^{-8}$ $cm^2\ s^{-1}$ [67% confidence intervals (CI), 6.6–9.1 $\times$ 10^{-8} $cm^2\ s^{-1}$], τ_M = 165 ns (CI, 152–173 ns), and τ_E = 63 ns (CI, 58–65 ns).

$$[\lambda J_1(\lambda R) + gJ_0(\lambda R)]Y_1(\lambda R_{max}) = [\lambda Y_1(\lambda R) + gY_0(\lambda R)]J_1(\lambda R_{max}) \quad (10)$$

where $g = \kappa/(2\pi DR)$; for each λ_n coefficient, $\gamma(\lambda_n)$ is calculated as

$$\gamma(\lambda_n) = -\frac{\lambda_n J_1(\lambda_n R) + gJ_0(\lambda_n R)}{\lambda_n Y_1(\lambda_n R) + gY_0(\lambda_n R)} = -\frac{J_1(\lambda_n R_{max})}{Y_1(\lambda_n R_{max})} \quad (11)$$

and coefficients $\alpha(\lambda_n)$ are defined by the uniform initial conditions:

$$\alpha(\lambda_n) = c\,\frac{\int_{R_0}^{R_1} r\{J_0(\lambda_n r) + \gamma(\lambda_n)Y_0(\lambda_n r)\}dr}{\int_{R_0}^{R_1} r\{J_0(\lambda_n r) + \gamma(\lambda_n)Y_0(\lambda_n r)\}^2\,dr},$$

$$n = 0, 1, \ldots \quad (12)$$

where $c = [\pi(R_{max}^2 - R^2)]^{-1}$.

The parameters of the model are the reaction radius R, the distance of maximum separation R_{max}, the diffusion coefficient D, the intrinsic rate constant κ; and the monomer decay time τ_M. In Ref. 32, it was shown that the global identifiability of this model requires a priori knowledge of the value of at least one the following parameters: R, R_{max}, D, or κ.

The excimer fluorescence intensity decay is represented by a convolution [33]:

$$E(t) = \exp\left(-\frac{t}{\tau_E}\right) \otimes \exp\left(-\frac{t}{\tau_M}\right)\left\{-\frac{dS(t)}{dt}\right\} \quad (13)$$

where $\otimes$ denotes convolution and τ_E is the fluorescence decay time of the excimer.

Data Analysis. As before, we apply the reference reconvolution method [see Eqs. (4) and (5)] to the analysis of monomer and excimer fluorescence decays. After combining Eqs. (4) and (8), the detected decay for the monomer via the fluorescence decay of the reference compound takes the form

$$F_M(t) = F_R(t) \otimes \left\{\left[\frac{1}{\tau_R} - \frac{1}{\tau_M}\right]M(t) + S(0)\exp\left(-\frac{t}{\tau_M}\right)\frac{dS(t)}{dt}\right\} + S(0)\,F_R(t) \quad (14)$$

From Eqs. (5) and (13), the detected excimer fluorescence profile is obtained as

$$F_E(t) = F_R(t) \otimes \left\{\left(\frac{1}{\tau_R} - \frac{1}{\tau_E}\right)E(t) - \exp\left(-\frac{t}{\tau_M}\right)\frac{dS(t)}{dt}\right\} \quad [15]$$

In the intramolecular model the survival probability $S(t)$ is equally present in the models for monomer [Eq. (8)] and excimer [Eq. (13)] emissions. Therefore, the parameters characterizing $S(t)$ (i.e., reaction radius R, maximum separation R_{max}, diffusion coefficient D, and intrinsic reaction rate constant κ) are the same for both decays, which implies the necessity of a global parametric fit of the fluorescence decay curves of monomer [Eq. (14)] and excimer [Eq. (15)] emission, assuming that the common parameters are equal for both curves.

Simulated Experiments. Here we explore how well two systems with different diffusion coefficients ($D = 3 \times 10^{-8}$ and 6×10^{-8} cm^2 s^{-1}) and the other parameters being equivalent ($R = 4 \times 10^{-8}$ cm, $R_{max} = 10^{-7}$ cm, $\kappa = 10^3$ cm s^{-1}, $\tau_M = 165$ ns, and $\tau_E = 60$ ns) can be distinguished by the fitting procedure, applied globally to the monomer and excimer kinetics, simulated with three values of signal-to-noise ratio (corresponding to 5×10^4, 10^5, and 5×10^5 counts in the peak channel).

The simulated model mimics the reference reconvolution method [21] with the reference decay time $\tau_R = 1.35$ ns, which was assumed to be known and fixed during the fit. According to the conclusions of the deterministic identifiability analysis [32], at least one of the parameters, D, R, R_{max}, or κ, must also be fixed. Thus, in fitting, we set the reaction radius R to its true value (4×10^{-8} cm). A typical example of simulated and fitted decay curves for a system with diffusion coefficient 3×10^{-8} cm^2 s^{-1} is presented in Fig. 3.

The results of simulated experiments are presented in Table I. The confidence intervals at the 67% level for the estimated values of parameters were obtained by the exhaustive search method [24]. One can see that the "statistical" identifiability of the diffusion coefficient can be achieved only under reasonably high values of signal-to-noise ratio. For example, with 5×10^4 counts in the peak channel, both diffusion coefficients are practically undistinguishable (their confidence intervals are highly overlapping). Relatively wide confidence intervals for parameters such as D, R_{max}, κ, and τ_M indicate that these parameters are strongly correlated: a change in one of them is well compensated by a change in the other ones, yet yielding a good quality of fit. Therefore, although the deterministic identifiabilty requires that only one parameter (in our case, it was R) must be fixed during the fit, in practice this might not be sufficient. The only parameter on which we can rely is the excimer decay time τ_E: the width of the confidence intervals for this parameter is almost negligible compared to that for the other parameters.

DISCUSSION

One important conclusion from both real and simulated decays is that one of the most significant parameters, the lateral diffusion constant (both long- and short-range), can be obtained within reasonable confidence boundaries

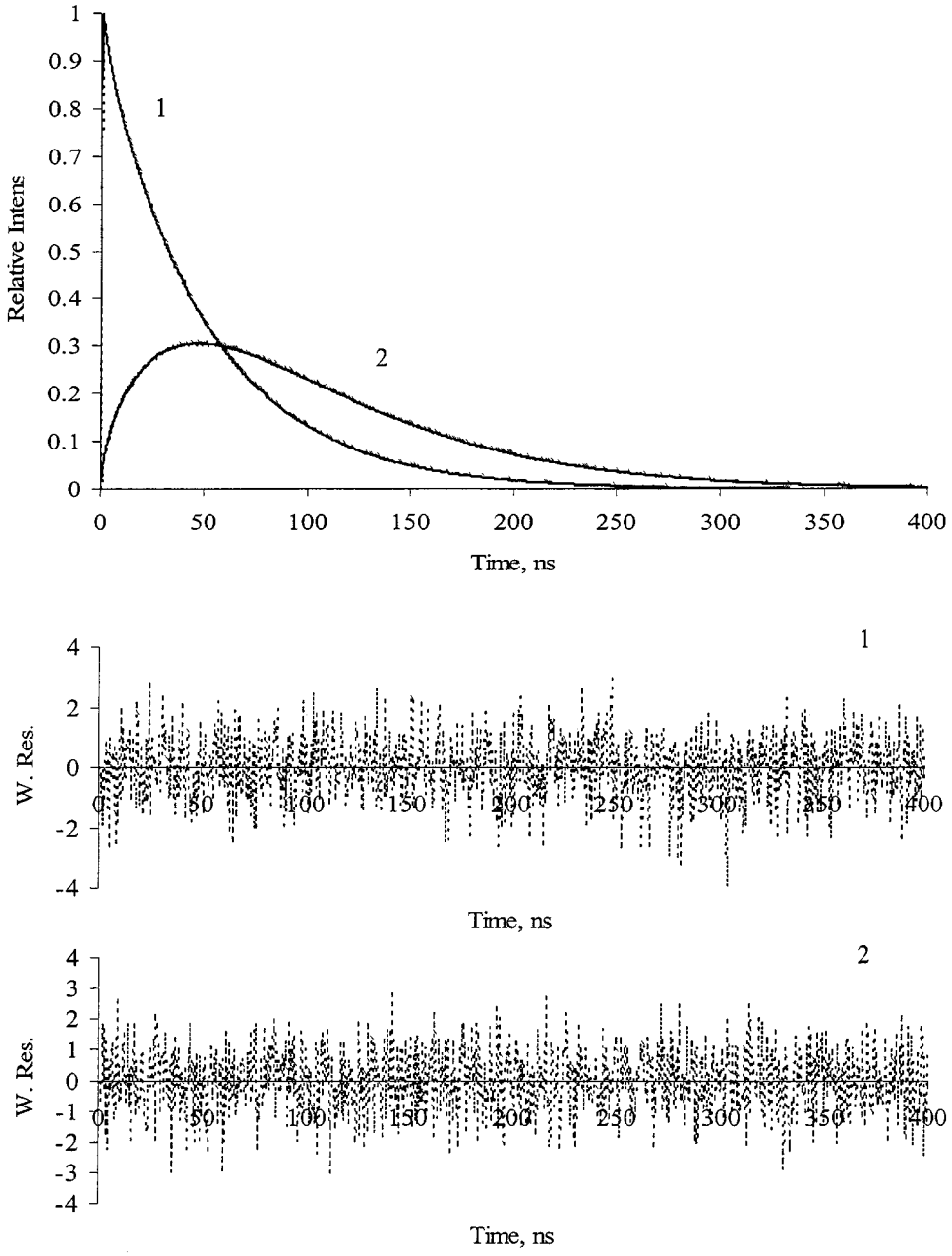

Fig. 3. Reference reconvolution of the time dependence of the monomer (curve 1) and excimer (curve 2) fluorescence of a simulated system with diffusion coefficient $D = 3 \times 10^{-8}$ cm^2 s^{-1}. Other parameters are listed in Table I. Simulated curves are represented by points and fitted curves by solid lines. The weighted residuals (W. Res.) for both globally analyzed curves (points) are also shown. The number of counts in the peak channel was 10^5; the number of time channels, 1000; and the width of each time channel, 0.4 ns.

when the experimental data have sufficient accuracy. When the time-correlated single-photon counting technique is used for pyrene-containing phospholipids in bilayer membranes, this would correspond to at least 10^5 photon counts in the peak channel.

It is noteworthy that the value of the translational diffusion coefficient recovered from analysis of the dipyrenyl derivative should not be compared to that derived from analysis of the monopyrenyl derivative. The value for the dipyrenyl case was taken rather arbitrarily, as the

Table I. Estimated Parameters of the Simulated "Intramolecular" System and Their Confidence Intervals at the 67% Level (Given in Square Brackets) for Two Values of the Diffusion Coefficient (3×10^{-8} and 6×10^{-8} cm^2 s^{-1}, Respectively) as a Function of the Number of Counts in the Peak Channel[a]

Peak channel	D (10^{-8} cm^2 s^{-1})	R_{max} (10^{-8} cm)	κ (cm s^{-1})	τ_M (ns)	τ_E (ns)
			$D = 3 \times 10^{-8}$ cm^2 s^{-1}		
$5 * 10^4$	3.21 [3.68; 1.63]	10.09 [14.12; 8.18]	1217.5 [15515.0; 430.0]	172.65 [226.61; 105.21]	60.01 [60.39; 59.64]
10^5	3.22 [3.81; 1.97]	10.16 [13.08; 8.70]	1416.4 [15721.6; 571.0]	169.37 [202.18; 119.62]	59.99 [60.37; 59.62]
$5 * 10^5$	3.11 [3.81; 2.63]	10.17 [11.61; 9.53]	1450.9 [5694.8; 838.8]	161.50 [180.68; 138.28]	60.00 [60.38; 59.63]
			$D = 6 \times 10^{-8}$ cm^2 s^{-1}		
$5 * 10^4$	5.99 [8.58; 2.17]	9.99 [15.11; 7.55]	1070.7 [11670.4; 391.5]	169.49 [529.66; 86.33]	60.07 [60.45; 59.70]
10^5	6.02 [8.73; 3.17]	9.97 [16.07; 8.16]	1016.8 [5338.0; 530.6]	178.75 [522.85; 95.52]	60.02 [60.40; 59.65]
$5 * 10^5$	6.03 [8.76; 4.82]	9.99 [13.61; 9.30]	999.4 [1986.4; 755.8]	171.41 [242.12; 98.03]	60.00 [60.38; 59.63]

[a] True values of the parameters are $\kappa = 10^3$ cm s^{-1}, $R_{max} = 10^{-7}$ cm, $\tau_M = 165$ ns, and $\tau_E = 60$ ns.

most important point was to demonstrate the quality of parameter recovery using simulated data. The values are expected to be different for intra- and intermolecular situations because of the different length scales involved for the two types of reactions.

There is an increasing demand to extrapolate the results obtained with a well-defined model system such as a homogeneous membrane bilayer to more complex systems such as the plasma membrane of a living cell. Can we use the same methodology to recover membrane fluidity gradients *in situ*? Such an approach implies that the current model has to be extended with a spatially dependent diffusion coefficient. Devising this model is not a simple task, as a closed mathematical solution is not expected and one has to rely on numerical methods to model the reaction kinetics. Then the advanced model must be tested on its parametric identifiability, but an experiment can always be arranged in such a way that the parameters of interest will be obtained with certain confidence by linking or fixing the other parameters. One should realize, however, that modeling of more complex systems such as the plasma membrane of a living cell requires more modifications than only spatially dependent diffusion coefficients.

A comprehensive overview of modeling reactions in biological membranes using pyrene excimer kinetics covering the literature up to the year 2000 is given in Ref. 34. Useful extensions are simulations using the Monte Carlo method for analyzing the kinetics of a diffusion-controlled irreversible bimolecular reaction and to compare the consistency of the simulated results with that of the experimental results of the pyrene excimer reaction [35]. The same authors have also developed some recipes for analyzing diffusion-controlled reactions in two dimensions with an eye toward the pragmatics of data analysis [36].

REFERENCES

1. T. Förster and K. Kasper (1955) *Z. Elektrochem.* **59**, 976.
2. H.-J. Galla and E. Sackmann (1974) *Biochim. Biophys. Acta* **339**, 103.
3. A. J. W. G. Visser (1997) *Curr. Opin. Colloid Interface Sci.* **2**, 27.
4. J. Eisinger, J. Flores, and W. P. Petersen (1986) *Biophys. J.* **57**, 987.
5. M. Sassaroli, M. Vauhkonen, D. Perry, and J. Eisinger (1990) *Biophys. J.* **49**, 281.
6. E. H. W. Pap, A. Hanicak, A. van Hoek, K. W. A. Wirtz, and A. J. W. G. Visser (1995) *Biochemistry* **34**, 9118.
7. K. Razi Naqvi (1974) *Chem. Phys. Lett.* **28**, 280.
8. J. Martins, W. L. Vaz, and E. Melo (1996) *J. Phys. Chem.* **100**, 1889.
9. E. G. Novikov, N. V. Visser, V. G. Malevitskaia, J. W. Borst, A. van Hoek, and A. J. W. G. Visser (2000) *Langmuir* **16**, 8749.
10. M. Vauhkonen, M. Sassaroli, P. Somerharju, and J. Eisinger (1990) *Biophys. J.* **57**, 291.
11. K. H. Cheng, S. Y. Chen, P. Butko, B. W. van der Meer, and P. Somerharju (1991) *Biophys. Chem.* **39**, 137.
12. M. Sassaroli, M. Vauhkonen, P. Somerharju, and S. Scarlata (1993) *Biophys. J.* **64**, 137.
13. L.-I. Liu, K. H. Cheng, and P. Somerharju (1993) *Biophys. J.* **64**, 1869.
14. K. H. Cheng, L. Ruymgaart, L.-I. Liu, P. Somerharju, and I. P. Sugar (1994) *Biophys. J.* **67**, 902.
15. K. H. Cheng and P. Somerharju (1996) *Biophys. J.* **70**, 2287.
16. E. H. W. Pap, P. A. W. van den Berg, J. W. Borst, and A. J. W. G. Visser (1995) *J. Biol. Chem.* **270**, 1254.
17. A. Szabo (1989) *J. Phys. Chem.* **93**, 6929.
18. M. Hauser and G. Wagenblast (1983) in R. B. Cundall and R. E. Dale (Eds.), *Time-Resolved Fluorescence Spectroscopy in Biochemistry and Biology*, Plenum Press, New York.
19. H. S. Carslaw and J. C. Jaeger (1959) *Conduction of Heat in Solids*, Oxford University Press, New York.
20. M. N. Berberan-Santos and J. M. G. Martinho (1992) *Chem. Phys.* **164**, 259.
21. K. Vos, A. van Hoek, and A. J. W. G. Visser (1987) *Eur. J. Biochem.* **165**, 55.
22. P. R. Bevington (1969) *Data Reduction and Error Analysis for the Physical Sciences*, McGraw–Hill, New York.

23. J. T. Edward (1970) *J. Chem. Educ.* **47**, 261.
24. J. M. Beechem, E. Gratton, M. Ameloot, J. R. Knutson, and L. Brand (1991) in J. R. Lakowicz (Ed.), *Topics in Fluorescence Spectroscopy, Vol. 2*, Plenum Press, New York.
25. D. Axelrod, D. E. Koppel, J. Schlessinger, E. Elson, and W. W. Webb (1976) *Biophys. J.* **16**, 1055.
26. M. Bloom and J. L. Thewalt (1994) *Chem. Phys. Lipids* **73**, 27.
27. P. Devaux and H. McConnell (1972) *J. Am. Chem. Soc.* **94**, 4475.
28. M. J. Saxton and K. Jacobson (1997) *Annu. Rev. Biophys. Biomol. Struct.* **26**, 373.
29. T. Schmidt, G. J. Schütz, W. Baumgartner, H. J. Gruber, and H. Schindler (1995) *J. Phys. Chem.* **99**, 17662.
30. M. Karplus and D. L. Weaver (1979) *Biopolymers* **18**, 1421.
31. G. Adam and M. Delbrück (1968) in A. Rich and N. Davidson (Eds.), *Structural Chemistry and Molecular Biology*, W. H. Freeman, San Francisco, pp. 198–215.
32. E. G. Novikov, A. Molski, and N. Boens (2000) *J. Chem. Phys.* **112**, 5348.
33. M. N. Berberan-Santos and J. M. G. Martinho (1991) *Chem. Phys. Lett.* **178**, 1.
34. J. M. Martins (2000) *On Modeling Reactions in Biological Membranes: Diffusion-Controlled Kinetics in Homogeneous Phospholipid Bilayers*, Ph.D. thesis, ITQB, Oeiras, Portugal.
35. J. Martins, K. Razi Naqvi, and E. Melo (2000) *J. Phys. Chem. B* **104**, 4986.
36. K. Razi Naqvi, J. Martins, and E. Melo (2000) *J. Phys. Chem. B* **104**, 12035.